New support structures for reduced overheating on downfacing regions of direct metal printed parts

Paggi, Umberto; Ranjan, Rajit; Thijs, Lore; Ayas, Can; Langelaar, Matthijs; van Keulen, Fred; van Hooreweder, Brecht

Publication date
2019

Document Version
Final published version

Published in
Proceedings of the Annual International Solid Freeform Fabrication Symposium

NEW SUPPORT STRUCTURES FOR REDUCED OVERHEATING ON DOWNFACING REGIONS OF DIRECT METAL PRINTED PARTS

Umberto Paggi[1,2,3], Rajit Ranjan[4],Lore Thijs[2], Can Ayas[4], Matthijs Langelaar[4], Fred van Keulen[4], Brecht van Hooreweder[1,3]

[1] KU Leuven, Department of Mechanical Engineering, Leuven, Belgium
[2]3D Systems Leuven, Belgium
[3]Member of Flanders Make - Core lab PMA-P, KU Leuven, Leuven, Belgium
[4]TU Delft, Department of Precision and Microsystems Engineering (PME), Delft, the Netherlands

Abstract

In Laser Powder Bed Fusion (LPBF), the downfacing surfaces usually have increased surface roughness and reduced dimensional accuracy due to local overheating and warpage. To partially overcome this a new supporting structure is developed in this study, namely the contactless support. This is a thin blade parallel to the critical area which transfer the heat away from the melt pool via conduction through the powder bed instead of direct contact. The support is tested in different geometries and printing conditions to define the optimal distance from the part and its effectiveness is evaluated by measuring the surface roughness of the samples. Numerical modelling of heat transfer phenomenon is also employed to determine the thermal history of the printing process and understand which parameters define the optimal distance for the thermal supports. Finally topology optimization is used to create a support structure which minimize the wasted material while keeping the heat flow optimal.

1. Introduction

The additive manufacturing (AM) market has been steadily growing in the last decade thanks to the ability of these techniques to produce near net shape components which are difficult or impossible to obtain with conventional production. This concept of complexity for free, as in the possibility to produce intricate parts without a significant increase in costs, is a popular term in literature, but to keep improving the design freedom there are still some limitations that need to be addressed.

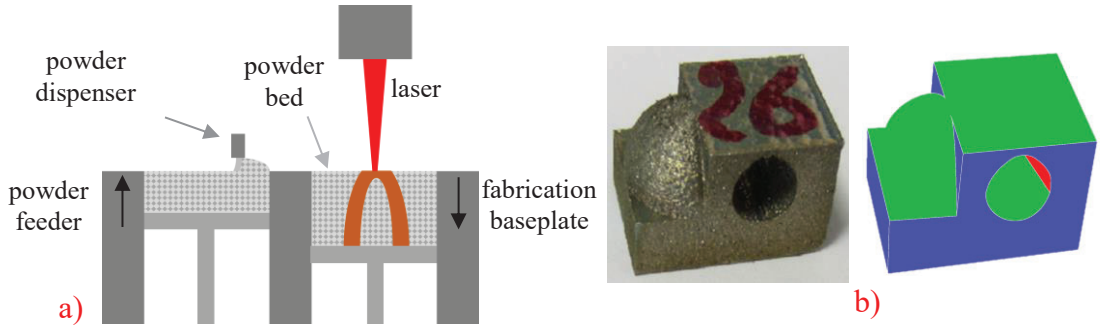

Fig. 1: a) Schematics of the LPBF process. b) Different types of surface in a general complex geometry. Upfacing areas are highlighted in green, vertical surfaces in blue and downfacing regions in red.

In the Laser Powder Bed Fusion the layers of powder are deposited and scanned by a laser one after the other to create the cross section of the desired geometry (Fig. 1a-b). In a general geometry it is possible to identify three main type surfaces which are upfacing, downfacing and vertical (Fig 1c). Upfacing and downfacing, as defined by the ISO/ASTM DIS 52911-1, are surfaces which normal vectors are, respectively, positive and negative in relation to the baseplate plane. Vertical surfaces, instead, are at 90° with the baseplate plane.

Regarding metal 3D printing one of the most challenging features are downfacing surfaces. While upfacing and vertical areas are scanned on top of bulk metal, downfacing regions are created on top of loose powder which negatively affect the printing quality in different ways. In general the powder material has a conductivity which is roughly one order of magnitude lower than the bulk metal, which leads to localized overheating and increased melt pool dimension (Fig 2a-b) [1]. Moreover, the powder bed cannot adequately support the liquid metal and because of gravity, capillarity, turbulent fluid flow and other phenomena the resulting melt pool is more instable and prone to defects (Fig 2c-d-e) [2]. These problems typically create drosses and sag on the downfacing region that negatively affect the surface roughness [1,3]. Furthermore, the geometrical accuracy of these areas is lower, compared to a middle section, because of warping and distortions that can happen on unsupported and overhanging sections (Fig 2f-g) [4,5,6]. This can be a major problem for small and detailed features, or complex geometries with unreachable downfacing, because the dimensional error can be larger than the tolerances required and can lead to build failure [7,8,9].

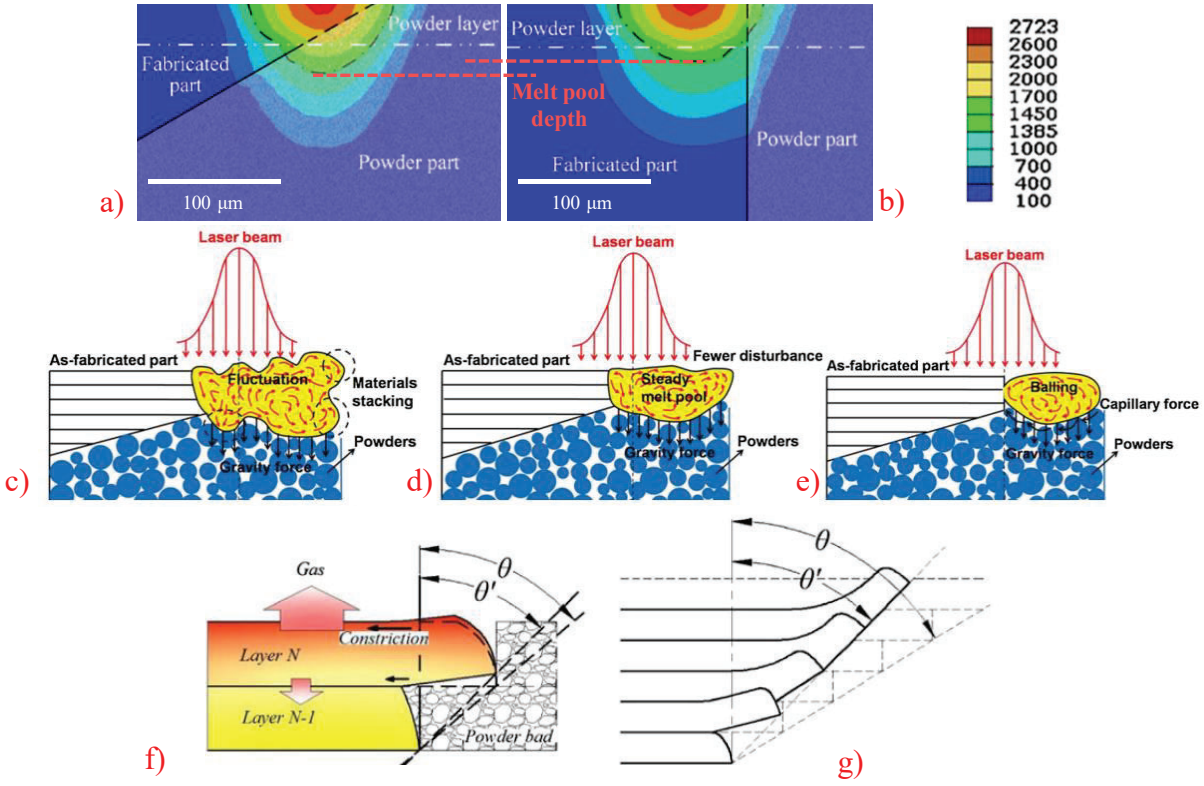

Fig. 2: Simulation of the thermal distribution for the same given process parameters on a) a downfacing geometry and b) on a vertical geometry [1]. Schematic of the melt pool flow with c) too high energy density, d) optimal energy density, and e) too low energy density [2]. Warping principle (f) and warping accumulation (g) during LPBF fabrication of overhanging surfaces [6].

The most common solutions that are employed to mitigate the problems introduced so far are the use of support structure and the tuning of process parameters in the downfacing area.

A first solution is the addition of supporting structures. Different structures can be built such as walls, lattices, cones, and so on. The main goal is either to provide heat conduction to the base plate, which act as a heat sink, or to mechanically stabilize the printed part, or both. Depending on the final purpose, these structures can be strongly or loosely attached to the sample and therefore can cause scarring and surface defect in the part, as can be seen in Fig 3 where a fragment of the support remained attached in the central area of the part in spite of being designed to be easily removed. These defects require different post processing steps to be removed and to achieve the final quality desired.

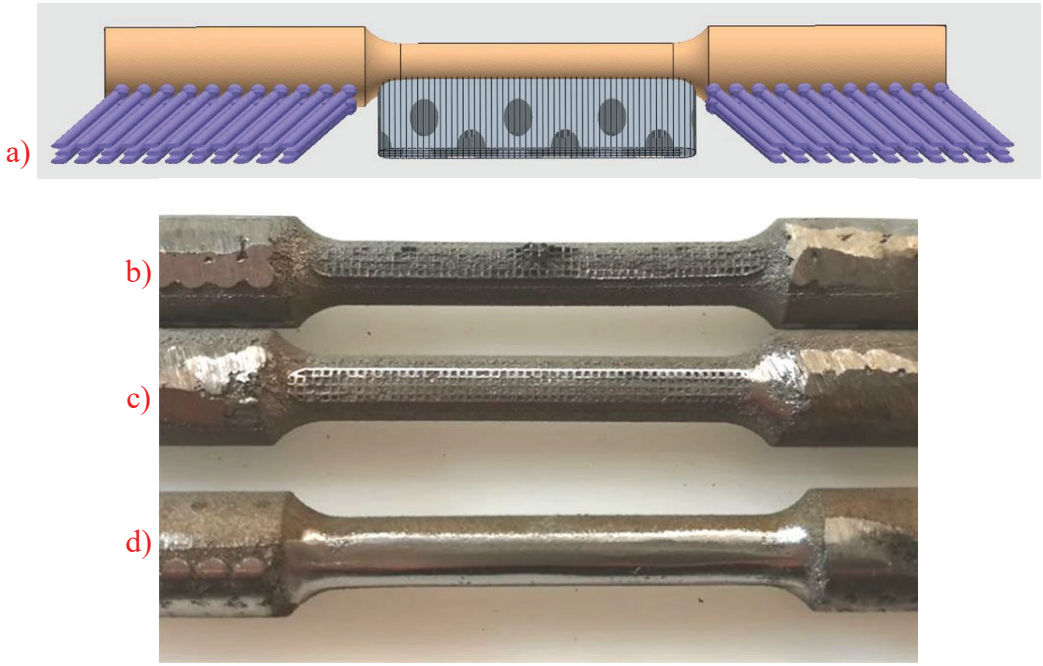

Fig. 3: a) CAD model of an horizontal tensile bar supported with a fine grid wall in the center to grant heat conduction, and cones on the sides to grant mechanical stability. b) Sample after manual removal of the supports. Part of the fine grid remains attached on the middle area, while on the sides the cones create a thick protruding. c) Sample after grinding to remove most of the excess material. d) Sample after polishing.

Another solution is to divide the printed part in two zones (Fig 4a), namely the fill zone which is printed over the bulk metal of the previous layer and the downfacing zone which is printed directly above (or few layers above) lose powder [10]. For each region the process parameters can be tuned in order to achieve the required properties (typically high relative density, low residual stresses, or high surface quality); in particular for the downfacing area a more stable weld track is generally obtained with lower energy densities [2] This also leads to smaller melt pools which prevent the formation of drosses (that can be several layers deep) and therefore increase the geometrical accuracy (Fig 4b-c-d-e).

Typically both strategies are employed on a complex geometry. Downfacing parameters are generally applied below 40-45° and can achieve a good enough surface quality and geometrical accuracy by themselves, depending on the area dimension, layer thickness, material properties, etc. Below 35-30° however the need for support structures becomes increasingly unavoidable, therefore

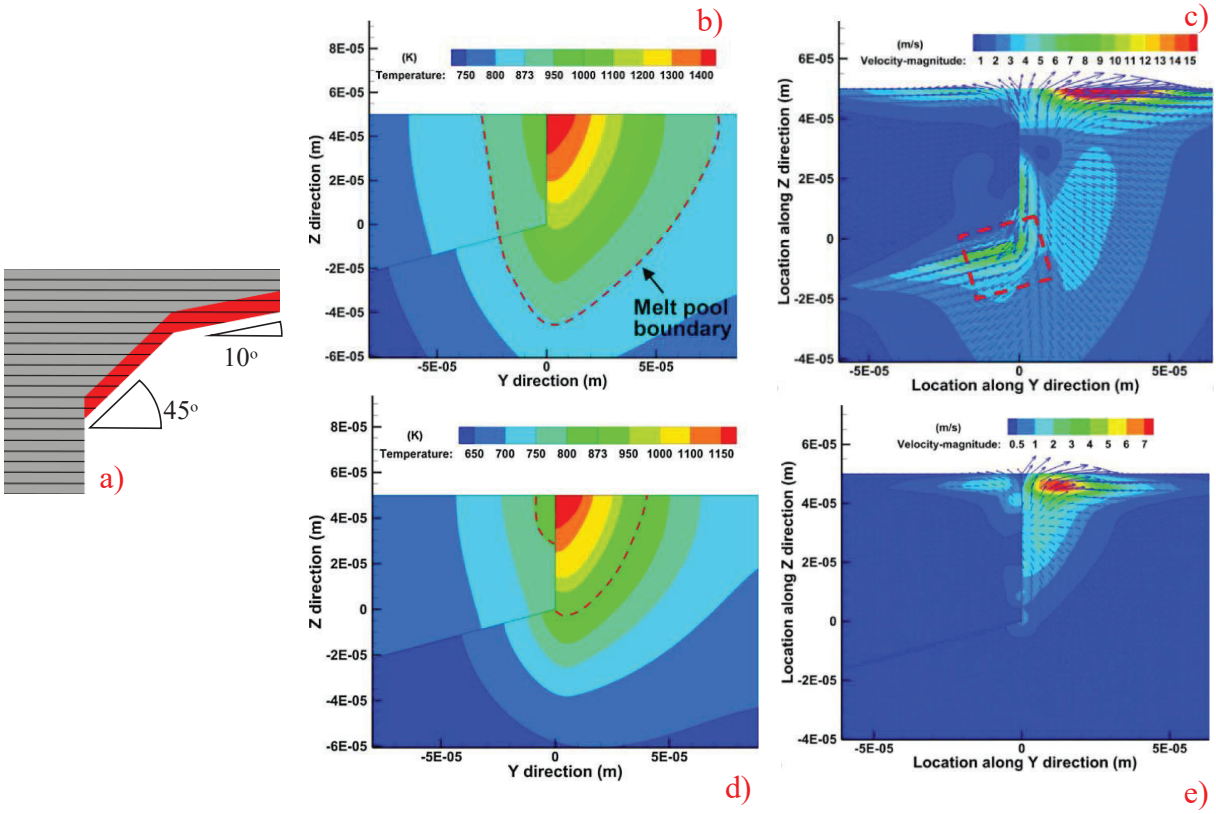

Fig. 4: a) Sample geometry in which downfacing parameters (in red) are applied for the first two layers printed over the powder bed. Simulation of the thermal distribution for a downfacing area printed with b) high energy density, and d) low energy density. Simulation of the melt flow for a downfacing area printed with c) high energy density, and e) low energy density. It is possible to notice how the liquid metal drips over the previous layer, worsening the surface quality[2].

In this paper a new way of supporting downfacing areas is studied, namely contactless support. Contactless support structures have already been tested for EBM technology in order to increase the geometrical accuracy of overhanging and sloped surfaces [11,12] (Fig 5a). Compared to the standard solution, these structures have the advantage of requiring very little effort in the removal step. The scarring of the printed part is also reduced to the minimum because very little conventional supports are needed to grant the mechanical stability required. In addition to these benefits, the contactless supports could improve the design freedom by reaching areas which cannot be post processed (Fig 5a): after the build is finished these structures could be easily detached and pulled out from the critical cavity while standard support would be unreachable.

This strategy has proven to be effective for samples of different shapes, dimensions and with different downfacing angles. However, previous literature focused only on reducing the distortion from the CAD model while the effect on surface topology was not characterized. Therefore in this paper different supporting condition and printing strategies will be tested in order to improve the surface quality of different downfacing areas.

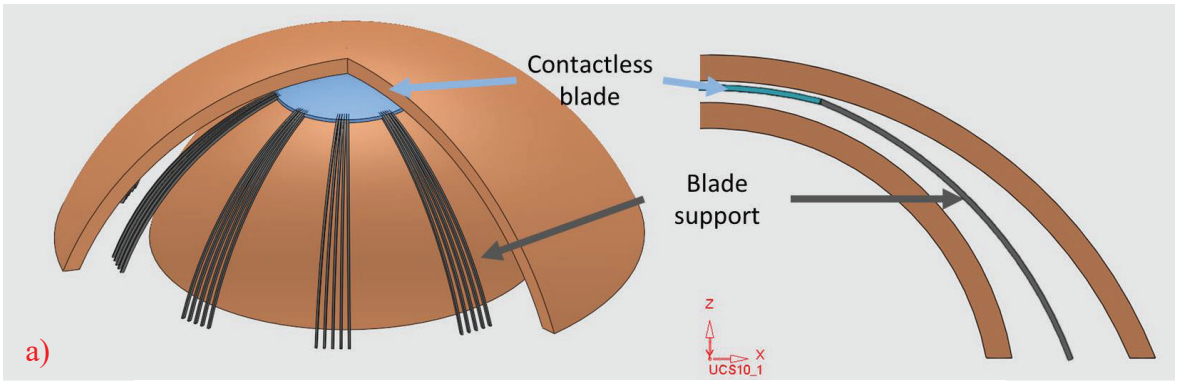

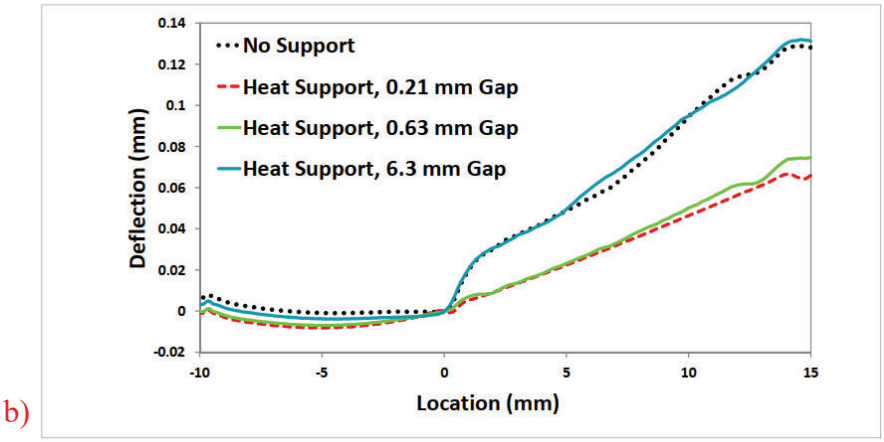

Fig. 5: a) Sample geometry with unreachable downfacing region. b) Deviation of overhanging cantilevers printed with and without contactless support with the EBM technique [12].

2. Materials and methods

In this study a series of downfacing samples are produced to evaluate the effectiveness of the contactless support as a substitute to conventional supports in term of heat extraction capabilities. Three types of downfacing samples are analyzed: flat overhangs, sloped downfacing at 45° and sloped downfacing at 30° (Fig 6). The geometries are designed with 3DXpert software provided by 3D Systems and printed in 30 µm, 60 µm and 90 µm layer thickness with a DMP Flex 350 in titanium powder LaserForm Ti Gr23 (A).

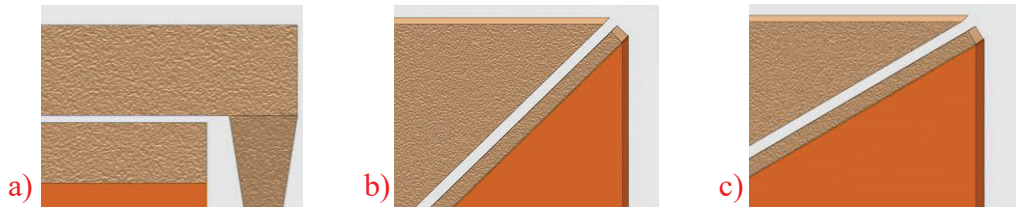

Fig. 6: Downfacing samples at a) 0°, b) 45°, and c) 30°.

Then, the optimal gap distance is found by printing various samples with increasing separation width for all three layer thicknesses, with a gap/layer thickness ratio ranging from 0.5 to 6 in 15-

20 um increments. The blade thickness is also varied from 200 μm to 1 mm. Three different printing strategies are tested:

1) The part is printed first, immediately followed by the contactless support
2) The contactless support is printed first, immediately followed by the part
3) The part is printed first, then a buffer time of 20 seconds is applied, and then the contactless support is printed

The surface roughness of the specimens is measured with a Taylor Hobson Form Talysurf 120L, with a 10 nm resolution. For each data point five measurements are performed and the average and standard deviation are reported. For the sloped downfacing samples the adequate acquisition length and filters (λ_c and λ_s) are selected according to the ISO 4287 (1997), ISO 4288 (1996) standards. On the contrary, on the flat overhang samples a maximum length of 8 mm is measurable, which is too short for the average roughness above 10 μm, typical for these structures. Nonetheless, according to Triantaphyllou et al. [13] a minimum length of 4 mm is enough to correctly asses the surface roughness of a sample, therefore the measurement is performed and the data is filtered according to the standards above.

3. Results and discussion

As a first step the supports for the thermal blade are optimized for high stiffness and heat conduction. This is a crucial aspect to guarantee stable and repeatable results because even small deformation in the contactless support can lead to welding with the main part, resulting in an irregular final surface. The final structure selected is a grid wall (Fig 7a-b), which grants a continuous and homogeneous supporting condition.

a) 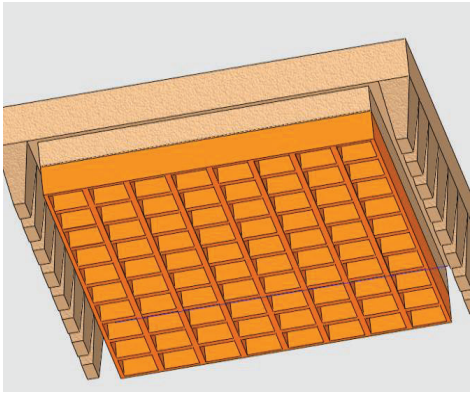 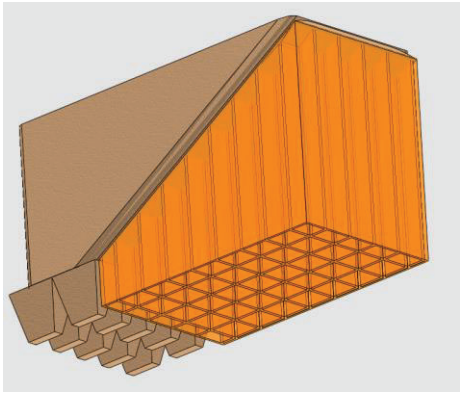 a)

Fig. 7: Grid support applied at the thermal blade on a) the flat overhang and b) sloped downfacing samples.

The next phase is the gap distance optimization. In this paper, we will only look to the effect of the contactless support on the surface roughness. The effect on the dimensional will be investigated in future work.

3. 1 Optimal gap distance in sloped downfacing

In Fig.8 the best results for the 30° samples with contact less supports are shown on the right side of each pair, while the reference samples are on the left side half as build and half sand blasted. For each combination of geometry and layer thickness the optimal gap distance was determined. The optimal gap distance is considered to be the smallest separation between the two structures for which no welding yet occurs.

It was observed that when the thermal blade is too far from the main part, the surface quality is largely unaffected and after the removal of the contactless support a considerable amount of loosely sintered powder remains attached to the downfacing region. At the optimal gap distance no sintered powder is left on the sample and the downfacing surface is regular and homogeneous. Below the optimal gap distance welding defects start to appear and the separation of the thermal blade form the sample becomes increasingly more difficult until the two parts are stuck together. As can be seen, the supported surfaces appear homogeneous and free of sintered powder, which instead is abundant in the as build reference condition. However, after sand blasting the surface roughness Ra value of the reference samples is lower than the supported ones, as noted In Table 1.

Regarding the effect of the angle of the sloped downfacing geometries, determining the optimal gap distance of the 30° sample was easier compared to the 45° sample. The latter samples, showed a less clear behavior with varying distance. Moreover, 45° is generally considered a non-critical downfacing angle which can go unsupported, so from now on it will be excluded from this study.

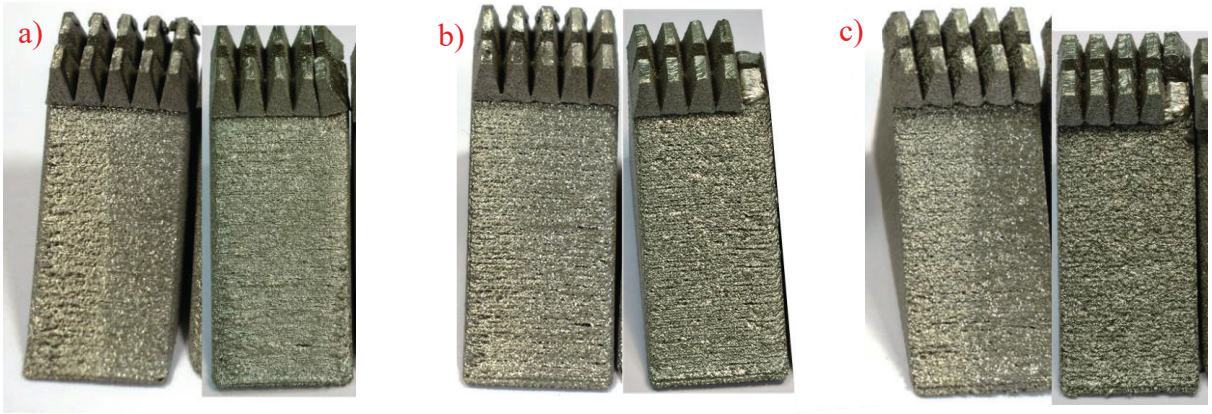

Fig. 8: Sloped downfacing samples at 30° printed in a) 30 µm, b) 60 µm, and c) 90 µm layer thickness.

	Ra/ µm		
	30 µm	60 µm	90 µm
Unsupported Sandblasted	15.22 +/- 1.12	18.13 +/- 0.79	21.99 +/- 1.22
Supported As built	17.90 +/- 1.18	20.06 +/- 1.32	24.66 +/- 2.03

Table 1: Surface roughness of the sloped samples. Each value is the average of five measurements and the standard deviation is used as error.

A likely explanation of this is a heat accumulation effect in the powder confined in the gap (Fig. 9a): as shown by Jamshidinia and Kovacevic [3] when two structures are printed close to each other the powder bed temperature increase (Fig.9 b-d). If they are close enough the temperature can become so high that partial sintering and melting occurs, increasing the surface roughness of the part. Moreover, hotter powder bed leads to bigger melt pool which once again are more instable and result in a lower quality surface.

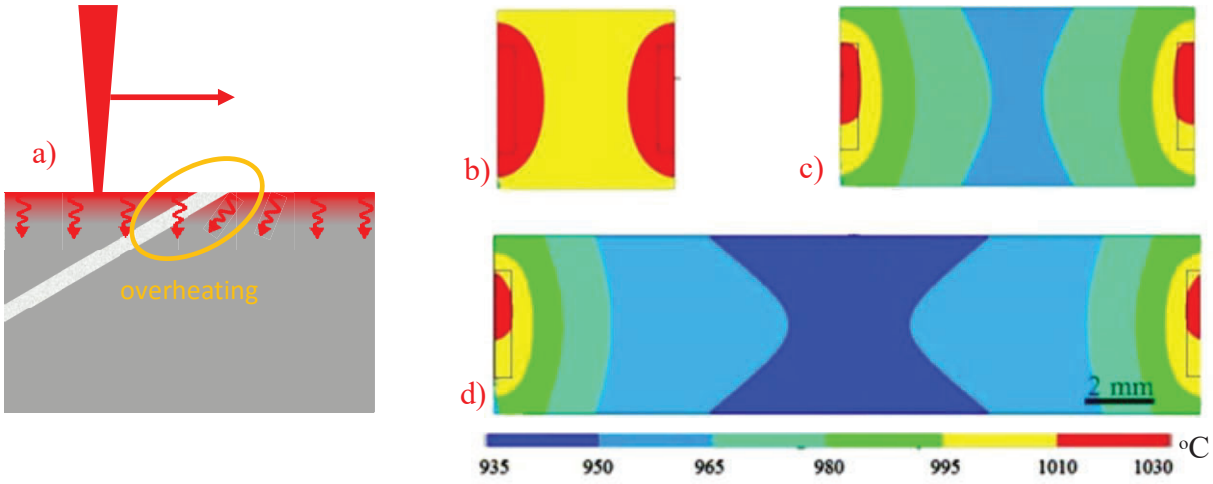

Fig. 9: a) Overheating in the powder gap of supported sloped downfacing samples. Comparison of temperature distributions during cooling at thin plates with different spacing distances of b) 5 mm, c) 10 mm, and d) 20 mm [3].

3. 2 Optimal gap distance in horizontal overhangs

Regarding the flat overhangs, a substantial improvement is achieved with the thermal support. In Fig. 10 samples in 30 µm, 60 µm and 90 µm layer thickness are shown which are produced unsupported (above) and with the employment of the thermal support (below). The reference surfaces are half sand blasted. For small geometries (1 cm x 1 cm) the downfacing region is self-supporting enough that the qualitative difference in surface texture between the two cases is small, especially after the sintered powder is removed with sand blasting from the unsupported sample.

For bigger geometries (2 cm x 2 cm), however, the stabilization effect of the contactless support is significantly larger. While the unsupported reference sample is completely warped, the contactless supported overhang remained flat. In Table 2 the values of the surface roughness measured on these horizontal downfacing areas are shown. The Ra value is not significantly affected regardless of the major improvement in surface flatness. On average, the Ra values of contactless supported samples are slightly higher than the reference ones. Therefore the contactless support open the possibility of creating parts with large flat downfacing areas in close geometries that would otherwise require a redesigning process, at the expenses of a slightly rougher but very homogeneous surface quality.

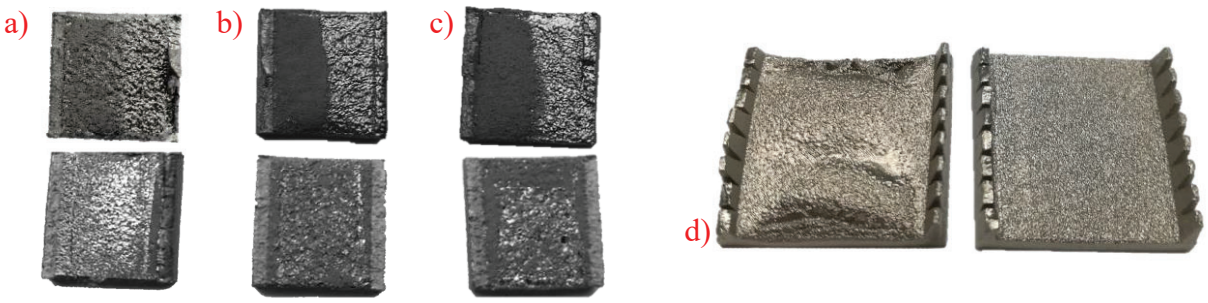

Fig. 10: Flat overhang samples of 1cm² area printed in a) 30 µm, b) 60 µm, and c) 90 µm layer thickness. d) Flat overhang samples of 4cm² area printed in 30 µm layer thickness.

	Ra/ µm		
	30 µm	60 µm	90 µm
1 cm x 1 cm Unsupported, sand blasted	10.92 +/- 1.12	39.35 +/- 2.51	15.97 +/- 1.07
1 cm x 1 cm Supported, as built	13.90 +/- 1.02	30.12 +/- 2.34	17.52 +/- 1.19
2 cm x 2 cm Unsupported, sand blasted	14.64 +/- 2.25	-	-
2 cm x 2 cm Supported, as built	16.98 +/- 0.96	-	-

Table 2: Surface roughness of the flat overhanging samples. Each value is the average of five measurements and the standard deviation is used as error.

3. 3 Sloped and horizontal downfacing comparison

Compared to the sloped downfacing samples, another positive aspect of the thermally supported overhangs is that the optimal gap distance is much more stable and does not vary for different dimensions or other printing conditions (position on the baseplate, time between layers, etc.).

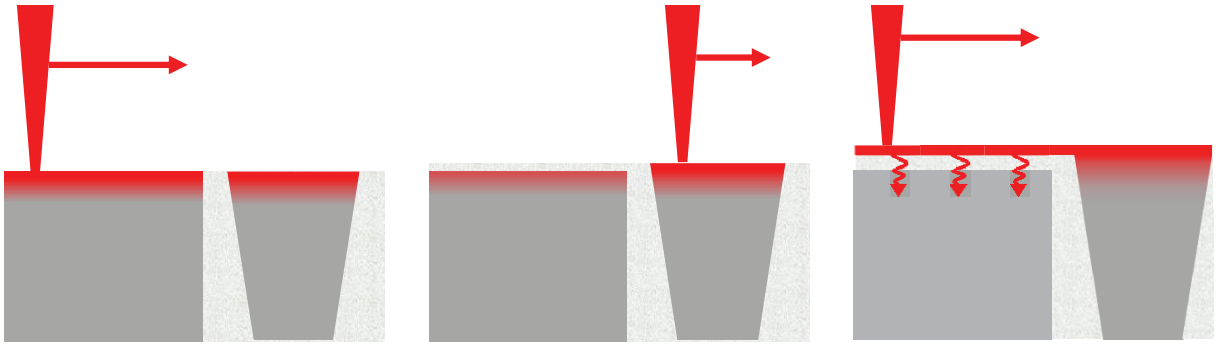

Fig. 11: Heat dissipation mechanism in the flat overhang samples

As stated above, this is probably linked to the heat accumulation in the gap powder. While for the sloped downfacing the particles are heated from both sides, in the flat overhangs the blade has enough time to cool down before the actual part is printed. Therefore the cold powder bed can

efficiently absorb and conduct the heat to the thermal blade, which in turn transfers it to the baseplate without overheating (Fig. 11).

To prove this hypothesis three other sloped series are produced, two with different printing strategies and one with a thicker thermal blade. In the first series the support is printed before the part because, being smaller, it should overheat less the surrounding powder. In the second series a printing buffer time is added between the main part and the thermal blade to let the heat diffuse towards the baseplate. In the third series a thicker blade is used which could act as local heat sink before the heat is transferred away. In Table 3 the results for these tests are shown: while thickening the blade or switching the printing order between the part and the support doesn't affect the gap at all, a slight improvement is seen when the powder is let to cool down. Specifically, the optimal gap distance was 10-20 micron shorter compared to the standard printing strategy, while the surface roughness remained constant.

	Δ optimal gap/µm		
	30 µm	60 µm	90 µm
Support/part	0	0	0
Part/buffer/support	0	0	0
Thicker blade	20	10	10

Table 3: Optimal gap distance change with different printing strategy and support condition.

This means that the thermal support can effectively extract the excess heat form the powder bed next to the downfacing area, but the transfer is slow and requires a minimum time to do so. If this prerequisite is met the overheating effect is mitigated and the welding phenomena (sintering and irregularly big melt pools that reach the support structure) start to appear at closer range, thus reducing the optimal gap distance.

3.4 Identification of critical parameters using thermal modelling

Optimizing the gap distance in an empirical way means a cost in term of time and resources, and the results are valid only for a specific geometry and printing condition. Therefore, to reduce the experimental load and to improve the flexibility of the contactless support, a thermal model is developed in Matlab to predict the severity of the overheating in a given geometry.

For this purpose, a transient thermal model is considered which is an abstract representation of the heat transfer phenomenon occurring within the sample. Fig. 12 shows multiple configurations where the domain is divided into three regions. The top, middle and bottom represents the part, the gap and the blade, respectively. The part and blade are assigned approximate solid thermal properties of Ti6Al4V whereas gap has been assumed to have powder properties as mentioned in [1]. Lastly, the domain is subjected to boundary conditions which are similar to AM process i.e. part is subjected to a surface heat load for 0,1s and then load is removed and it is allowed to cool down for next 2s. The bottom of the domain is fixed at a constant temperature acting as an ideal heat sink emulating the thermal effect of substrate plate and only conduction is considered. It is important to notice that the results shown in this paper are not representative of the real temperature reached by the process, but rather are a relative measure of the capability of the support to extract heat from the printed part.

Different configurations of the contactless support were tested. First of all the shape of the blade was varied from a flat surface to a spiked one, while maintaining the average distance from the printed part constant. The resulting maximum temperature graph shows that this configuration worsen the heat exchange rate and creates an inhomogeneous temperature distribution which could lead to pattern and unwanted topology on the final surface. The thickness of the support was also varied while keeping the gap dimension constant and this resulted in exactly the same temperature profile, which suggest that the main factor in the heat extraction problem (as long as the blade starting temperature is T_0) is the powder gap.

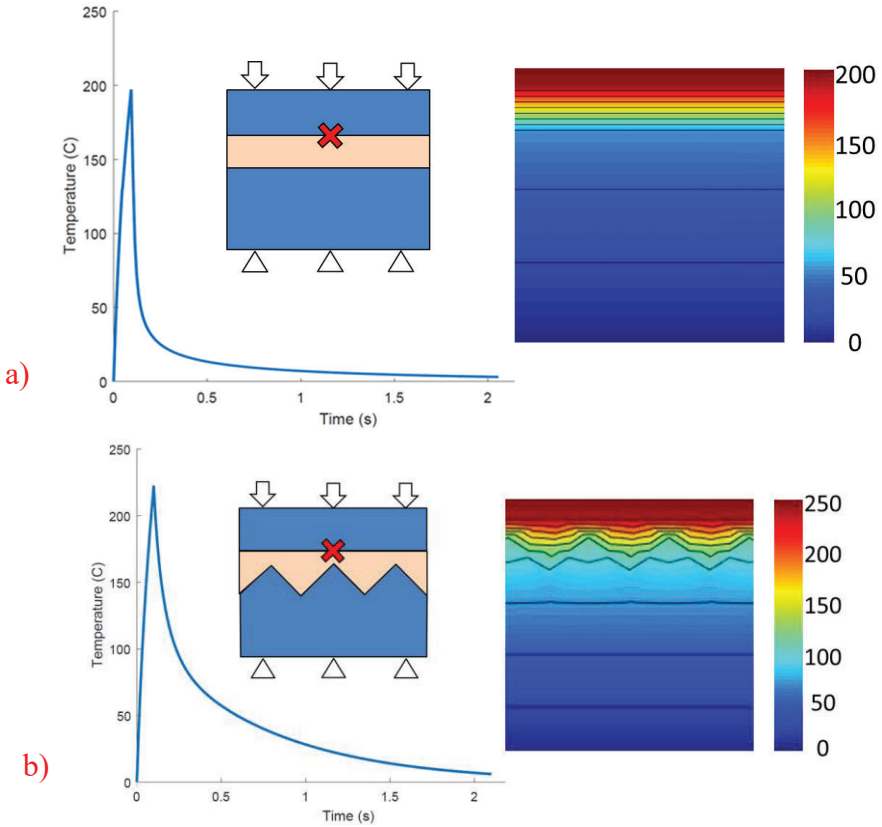

Fig. 12: Thermal simulation of the contactless support with a) a flat blade, and b) a spiked blade. It is clear that the second one creates a less homogeneous temperature distribution.

Therefore, another simulation was performed varying the gap width (Fig. 13) and the results show that the maximum temperature reached is directly linked to this parameter. This could mean that when we have little powder the heat is quickly dissipated to the support structure and this should prevent any sintering or partial melting of the particle which leads to welding and attachment. Hence, the main factor to keep in mind when optimizing the gap width should be the melt pool depth, which leads to welding when the gap dimension is smaller than that.

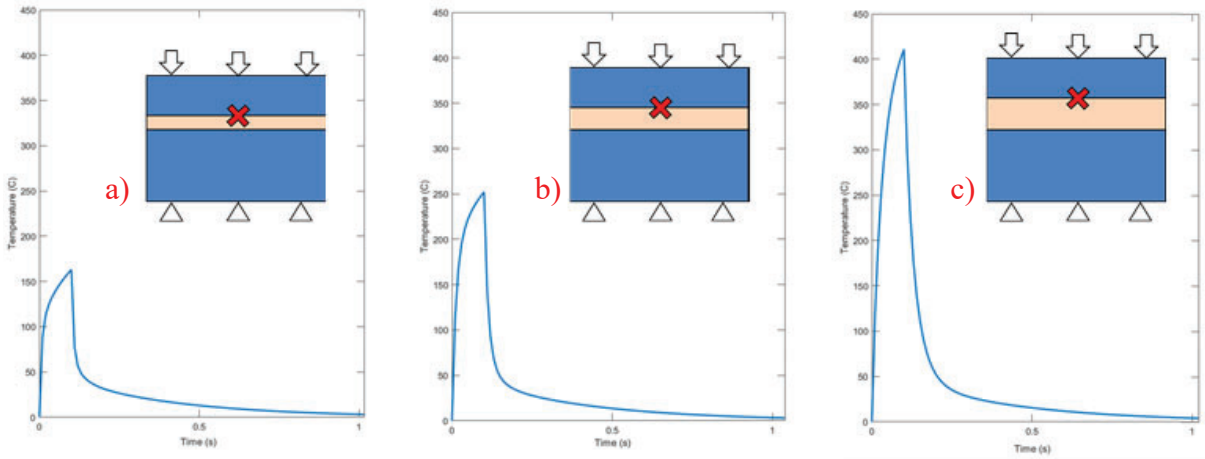

Fig. 13: Thermal simulation of the contactless support with varying gap width of a) 100 µm, b) 200 µm, c) and 400 µm.

3.5 Topology optimization for finding thermally efficient supports

A simplified AM model as presented by Ranjan et al. [14] has been used to define thermal loading for finding optimal supports. The model is referred to as 'hotspot indicator' and shown to be able to identify zones of local heat accumulation in a given part geometry. In this research, we first run the model on the fixed part to identify critical zones from the context of overheating. Then, an optimization is carried out such that these identified critical zones are adequately connected to the substrate ensuring heat evacuation. For this purpose, a flux boundary condition is defined using the hotspot while bottom of the domain is fixed as a heat sink. The part is considered a non-design domain and topology optimization is performed to find the supports that minimize the thermal compliance. Fig. 14a shows a sample geometry (L shape) with long overhang. The temperature field obtained from the hotspot analysis is imposed on the part which gives an indication of maximum temperature obtained during the build process, assuming no supports are used. As expected, the region close to overhangs are identified as a source of overheating, with the effect increasing with the length of overhanging feature. The result of the minimum thermal compliance optimization problem has been shown in Fig. 14b, which presents the final optimized supports. As it can be noticed, the topology optimization delivers a structure that penetrate the initial geometry. This happens because the best way to transfer heat from the part to the support is physical contact and no consideration has been made to avoid this. This is problematic because, first of all, two objects cannot occupy the same volume and secondly that the junction between support and geometry need to be as low as possible to allow for an easy separation and surface finishing at the end of the building process.

Therefore, a weight factor is introduced which disfavor the amount of surface in common between support and printed part. The obtained structure is shown in Fig 14 c-d. The result shows the found design for permissible volume fraction of 10% and 50%. This factor is set as a priority and can vary based on the structural requirement of the supports and the heat extraction target for the overall geometry. It is observed that to reduce the contact area between part and the support, the adapted algorithm assign a density value at the interface, represented by gray pixels. This is a common occurrence in topology optimization problems where intermediate density is used to relax the discrete nature of optimization. Recently an interpretation of this result was proposed where

the gray areas are realized as scaffold structures with the corresponding relative density [15]. This is indeed reflected in the industrial practice where scaffolds are often employed as support structures, but another way to realize it could be to use the concept of contactless support proposed in this paper. Since the powder bed has in fact a density lower than the maximum density of the bulk metal, by matching the heat transfer of the gap with the one corresponding to the optimized structure a new support could be created that efficiently remove heat from the downfacing surfaces. This promotes a homogeneous boundary condition resulting in a more regular surface, and prevents the creation of scars and defects associated with support removal that would require extra post processing steps.

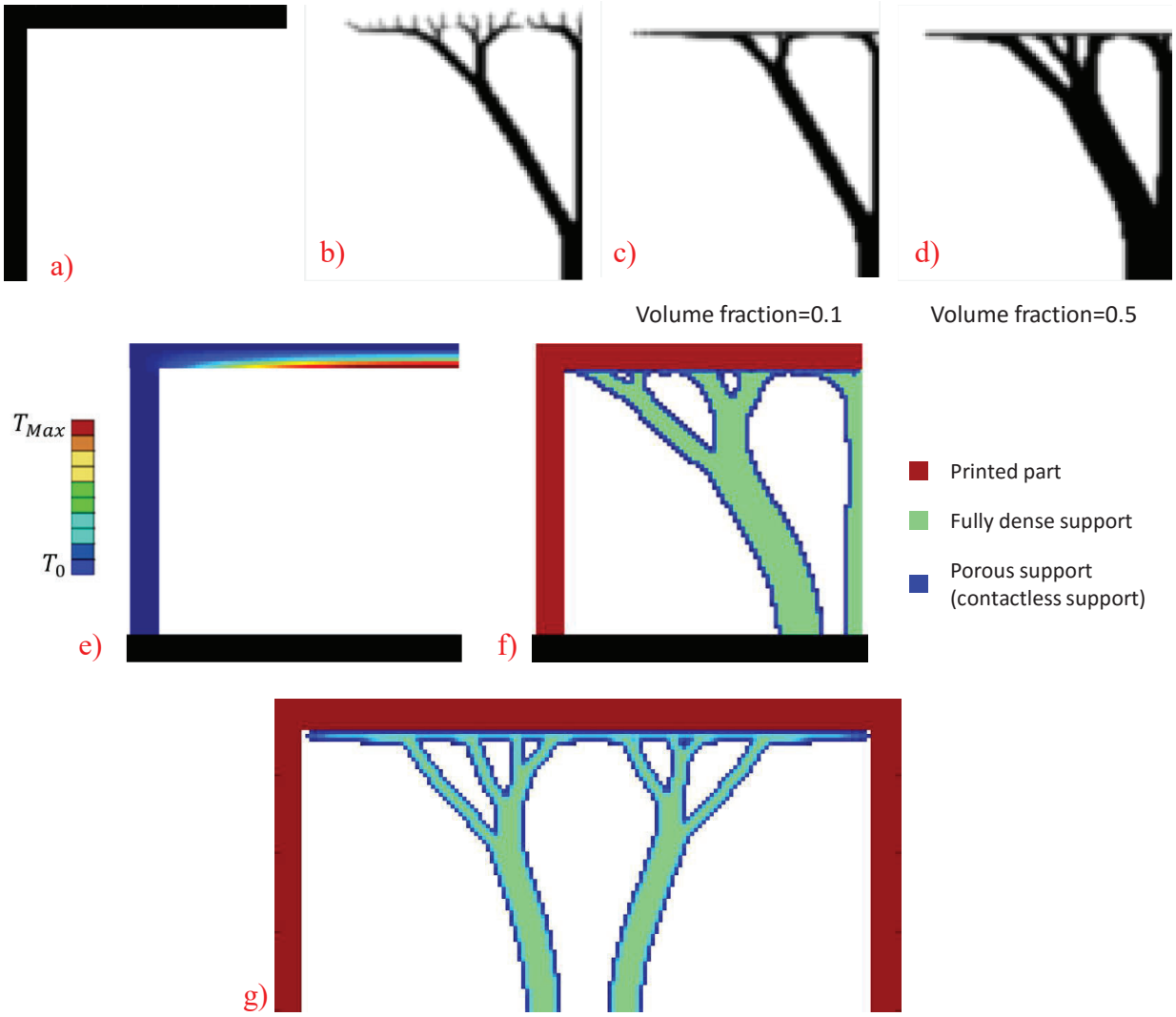

Fig. 14: a) Sample overhanging geometry. b) Topology optimization result for the best heat extraction support. Topology optimization result, with weight factor for minimal contact, for the best heat extraction support with c) 10% permissible volume fraction and d)50% permissible volume fraction. e) Hot spot indicator results for the sample overhanging geometry. f) Representation in colors of the topology optimization result, with weight factor for minimal contact, for the best heat extraction support. g) Topology optimization result, with weight factor for minimal contact, for a bridge overhanging geometry.

4. Conclusions and future studies

In this paper the feasibility of a new contactless support structure is investigated comparing the surface quality and geometrical accuracy in reference sample produced unsupported and sandblasted, and in supported samples as built. Both via modeling as well as experimentally, it was observed that the thickness of the powder gap has the largest influence on the improvement of the surface quality.

From the three considered downfacing angles, 0°, 30° and 45°, the 0° or horizontal down-facing surfaces were most significantly impacted. Although the Ra value did not improve, a dramatic impact on the flatness of the surfaces was obtained for surfaces as large a 2 x2 cm. The application of the contactless support showed the capability of reducing significantly warping of these surfaces.

Next to the experimental exploration of the capability of these contactless supports, also topology optimization methods were created in this work in order to be able to design these new support structures for more complex parts.

The authors are very hopeful that in the future complex designs that normally couldn't be printed because of large critical downfacing areas could be printed by the use of these topologically calculated thermal blades

5. Acknowledgments

This research was funded by The EU Framework Programme for Research and Innovation - Horizon 2020 - Grant Agreement No 721383 within the PAM2 research project.

References

[1] Xiang, Z., Wang, L., Yang, C., Yin, M. & Yin, G. Analysis of the quality of slope surface in selective laser melting process by simulation and experiments. Optik 176, 68–77 (2019).
[2] Chen, H., Gu, D., Xiong, J. & Xia, M. Improving additive manufacturing processability of hard-to-process overhanging structure by selective laser melting. Journal of Materials Processing Technology 250, 99–108 (2017).
[3] Jamshidinia, M. & Kovacevic, R. The influence of heat accumulation on the surface roughness in powder-bed additive manufacturing. Surf. Topogr.: Metrol. Prop. 3, 014003 (2015).
[4] Cheng, B. & Chou, K. Deformation Evaluation of Part Overhang Configurations in Electron Beam Additive Manufacturing. Processing V001T02A072, ASME, Volume 1 (2015).
[5] Calignano, F. Design optimization of supports for overhanging structures in aluminum and titanium alloys by selective laser melting. Materials & Design 64, 203–213 (2014).
[6] Wang, D., Yang, Y., Yi, Z. & Su, X. Research on the fabricating quality optimization of the overhanging surface in SLM process. The International Journal of Advanced Manufacturing Technology 65, (2013).
[7] Pakkanen, J. et al. Study of Internal Channel Surface Roughnesses Manufactured by Selective Laser Melting in Aluminum and Titanium Alloys. Metall and Mat Trans A 47, 3837–3844 (2016).

[8] Snyder, J. C., Stimpson, C. K., Thole, K. A. & Mongillo, D. J. Build Direction Effects on Microchannel Tolerance and Surface Roughness. J. Mech. Des 137, 111411-111411–7 (2015).
[9] Atzeni, E. & Salmi, A. Study on unsupported overhangs of AlSi10Mg parts processed by Direct Metal Laser Sintering (DMLS). Journal of Manufacturing Processes 20, 500–506 (2015).
[10] Cloots, M., Zumofen, L., Spierings, A. B., Kirchheim, A. & Wegener, K. Approaches to minimize overhang angles of SLM parts. Rapid Prototyping Journal 23, 362–369 (2017).
[11] Cheng, B. & Chou, K. Deformation Evaluation of Part Overhang Configurations in Electron Beam Additive Manufacturing. in Volume 1: Processing V001T02A072 (ASME, 2015).
[12] Cooper, K., Steele, P., Cheng, B. & Chou, K. Contact-Free Support Structures for Part Overhangs in Powder-Bed Metal Additive Manufacturing. Inventions 3, 2 (2017).
[13] Triantaphyllou, A. et al. Surface texture measurement for additive manufacturing. Surf. Topogr.: Metrol. Prop. 3, 024002 (2015).
[14]Ranjan, R., Yang, Y., Ayas, C., Langelaar, M. & Keulen, F. Controlling Local Overheating in Topology Optimization for Additive Manufacturing. in (2017).
[15] Adam, G. A. O. & Zimmer, D. Design for Additive Manufacturing—Element transitions and aggregated structures. CIRP Journal of Manufacturing Science and Technology 7, 20–28 (2014).